

Ionization of hydrogen atoms by electron impact at 1eV, 0.5eV and 0.3eV above threshold

J. N. Das and S. Paul

Department of Applied Mathematics, University College of Science, 92 A. P. C. Road, Calcutta 700 006, India.

K. Chakrabarti*

*Department of Mathematics, Scottish Church College,
1 & 3 Urquhart Square, Calcutta 700 009, India*

(Dated: November 21, 2018)

We present here triple differential cross sections for ionization of hydrogen atoms by electron impact at 1eV, 0.5eV and 0.3eV energy above threshold, calculated in the hyperspherical partial wave theory. The results are in very good agreement with the available semiclassical results of Deb and Crothers [13] for these energies. With this, we are able to demonstrate that the hyperspherical partial wave theory yields good cross sections from 30 eV [12] down to near threshold for equal energy sharing kinematics.

PACS numbers: 34.80.Dp, 34.50.Fa

I. INTRODUCTION

Over the last couple of years considerable progress has been made in the study of ionization of hydrogen atoms by electron impact, apparently the simplest three body coulomb problem in quantum scattering theory, at low energies. Still full understanding of this problem, particularly near threshold, has not been achieved.

Ionization near threshold was studied by Pan and Starace [1] where they reported a distorted wave calculations of (e, 2e) process with H, He and other rare gas targets at excess energies 4 eV (above the respective ionization thresholds) and below for equal energy sharing kinematics. For atomic hydrogen they reported results at excess energies 2 eV and 0.5 eV above threshold in the coplanar constant θ_{ab} geometry (in which the angle θ_{ab} between the emerging electrons remain fixed) with $\theta_{ab} = \pi$. Jones, Madison and Srivastava [2] also reported a distorted wave (e, 2e) calculation with atomic hydrogen and helium target for equal energy sharing kinematics but different geometries. Their results were in good qualitative agreement with the experiments at 2 eV above threshold for atomic hydrogen for constant θ_{ab} geometries. However, for the other geometries presented, there were considerable deviations from the experimental results.

For equal-energy-sharing kinematics McCurdy and co-workers made a break-through calculation in their exterior complex scaling (ECS) approach [3, 4, 5]. Their results for 30eV, 25eV, 19.6eV and 17.6eV agree excellently with the measured results of Röder *et al* [6, 7, 8]. However, below 2eV, results of ECS theory are not yet available. Another sophisticated approach is the convergent close-coupling (CCC) theory of Bray and associates

[9, 10, 11], which works beautifully for many atomic scattering problems and reproduces ionization cross section results very satisfactorily above 2eV excess energy. For 2eV excess energy their results differ approximately by a factor of two from the absolute measured values [6]. Below 2eV excess energy CCC results are also not available. Recent calculations of Das and co-workers [12] for equal energy sharing kinematics in the hyperspherical partial wave (HPW) theory also reproduced the experimental data [6, 8] quite satisfactorily.

So far the hyperspherical partial wave theory has not been tested below 2eV excess energy. Deb and Crothers [13] have reported a semiclassical calculation that gives very good cross section results for low energies of 4eV and 2eV above threshold and also for energies 1eV, 0.5eV and 0.3eV above threshold. This calculation encouraged us to test whether the hyperspherical partial wave theory works for excess energy below 2eV. Here we made such a calculation for excess energy of 1eV, 0.5eV and 0.3eV above the ionization threshold. We found that the HPW theory gives cross section results in very good agreement with the semi classical calculation of Deb and Crothers [13] for the above energies. One only needs to increase the asymptotic range parameter R_∞ (defined later) to sufficiently large values of several thousands of a.u. It is interesting to note here that the hyperspherical \mathcal{R} -matrix with semiclassical outgoing waves (HRM-SOW) calculation of Selles *et al* [14], for the double photo-ionization of the Helium atom, also requires R_∞ values of several thousands of a.u. for converged results.

II. HYPERSPHERICAL PARTIAL WAVE THEORY

The hyperspherical partial wave theory has been described in details in [12, 15] and briefly in [17, 18]. In this approach we determine scattering amplitude from

*Electronic address: kkch@eth.net

the T-matrix element given by

$$T_{fi} = \langle \Psi_f^{(-)} | V_i | \Phi_i \rangle \quad (1)$$

where Φ_i is the initial state wave function, V_i is the interaction potential in this channel and $\Psi_f^{(-)}$ is the exact two-electron continuum wave function with incoming boundary conditions in presence of the nucleus, which is considered infinitely heavy and stationary at the origin. The scattering state $\Psi_f^{(-)}$ is determined by expanding it in terms of symmetrized hyperspherical harmonics [15, 19] which are functions of five angular variables. The hyperradius and the angular variables are defined by $R = \sqrt{r_1^2 + r_2^2}$, $\alpha = \arctan(r_2/r_1)$, $\hat{r}_1 = (\theta_1, \phi_1)$, $\hat{r}_2 = (\theta_2, \phi_2)$ and $\omega = (\alpha, \hat{r}_1, \hat{r}_2)$ and set $P = \sqrt{p_1^2 + p_2^2}$, $\alpha_0 = \arctan(p_2/p_1)$, $\hat{p}_1 = (\theta_{p_1}, \phi_{p_1})$, $\hat{p}_2 = (\theta_{p_2}, \phi_{p_2})$ and $\omega_0 = (\alpha_0, \hat{p}_1, \hat{p}_2)$, \vec{p}_1 , \vec{p}_2 being momenta of the two outgoing electrons of energies E_1 and E_2 , and positions \vec{r}_1 and \vec{r}_2 .

Different sets of radial waves with definite $\mu = (L, S, \pi)$, (where L is the total angular momentum, S is total spin and π is the parity) satisfy different sets of coupled equations each of the form

$$\left[\frac{d^2}{dR^2} + P^2 - \frac{\nu_N(\nu_N + 1)}{R^2} \right] f_N + \sum_{N'} \frac{2P \alpha_{NN'}}{R} f_{N'} = 0. \quad (2)$$

These equations are truncated to $N = N_{mx}$ which is the number of channels retained in the calculation for each fixed μ . The N_{mx} number of independent solutions of the truncated equations, need to be determined over the interval $(0, \infty)$. These equations may then be solved in different alternative approaches. One possibility is to partition this interval into three subintervals $(0, \Delta)$, (Δ, R_∞) and (R_∞, ∞) , Δ being of the order of a few atomic units and R_∞ being a point in the far asymptotic domain. The solution in $(0, \Delta)$ is then constructed as in

the R-matrix [16] method and then continued to R_∞ using Taylor's expansion method [17, 18]. Beyond R_∞ the solutions are known from series expansions [12]. This approach, however, suffers from pseudo resonance problems as pointed out in Ref. [18] and hence this is not the one adopted here. Other possibilities include solving the set of equations as a two point boundary value problem (since the radial wave function is known at origin, and at R_∞ from series expansions) as in the ECS method [4]. This again would require more computational resources than that we have at present. The most effective approach for our purposes turns out to be the following. We construct N_{mx} independent solutions of Eq. (2) over the interval $(0, \Delta)$ by solving these as a two-point boundary value problem. The k^{th} solution vector is made to vanish at the origin and takes the k^{th} column of the $N_{mx} \times N_{mx}$ unit matrix as its value at Δ . These solutions are then continued over (Δ, R_∞) by solving the coupled system of equations by the Taylor's expansion method with frequent stabilization [20]. Beyond R_∞ the solution may be obtained from expansion in inverse powers of R with suitable sine and cosine factors [12, 15]. The asymptotic incoming boundary conditions then completely define [12, 15] the scattering-state wave function $\Psi_{fs}^{(-)}$. For the initial interval $(0, \Delta)$ solution by the finite difference method proves most effective. In our earlier calculation [12], at higher energies we used a five-point difference scheme. This gives us very good cross sections for 30eV, 25eV, 19.6eV and 17.6eV for various kinematic conditions. In our present calculation we propose to use larger mesh size (double that of our previous calculation) and hence, in place of a five-point difference scheme we use a seven-point difference scheme. In the seven-point scheme we divide the interval $[0, \Delta]$ into m subintervals by using mesh points $R_0, R_1, R_2, \dots, R_{m-1}, R_m$ where $R_k = hk$, ($k = 0, 1, 2, \dots, m$) and $h = \Delta/m$. In this scheme we use the following formulae:

$$f_N''(R_k) = \frac{1}{h^2} \left[\frac{1}{90} f_N(R_{k-3}) - \frac{3}{20} 16 f_N(R_{k-2}) + \frac{3}{2} f_N(R_{k-1}) - \frac{49}{18} f_N(R_k) + \frac{3}{2} f_N(R_{k+1}) - \frac{3}{20} 16 f_N(R_{k+2}) \right. \\ \left. + \frac{1}{90} f_N(R_{k+3}) \right] + \left\{ \frac{69}{25200} h^6 f_N^{(viii)}(\xi_1) \right\} \quad (3)$$

for $k = 3, 4, \dots, m-4, m-3$. For $k = 1, 2$ and $m-2, m-1$

we use the the formulae

$$f_N''(R_1) = \frac{1}{h^2} \left[\frac{3}{8} f_N(R_0) + 6 f_N(R_1) - \frac{11}{2} h^2 f_N''(R_2) - \frac{51}{4} f_N(R_3) - h^2 f_N''(R_3) + 6 f_N(R_4) + \frac{3}{8} f_N(R_4) \right] \\ + \left\{ -\frac{23}{10080} h^6 f_N^{(viii)}(\xi_2) \right\}. \quad (4)$$

$$f_N''(R_2) = \frac{1}{h^2} \left[\frac{3}{8} f_N(R_1) + 6f_N(R_2) - \frac{11}{2} h^2 f_N''(R_3) - \frac{51}{4} f_N(R_3) - h^2 f_N''(R_4) + 6f_N(R_4) + \frac{3}{8} f_N(R_5) \right] + \left\{ -\frac{23}{10080} h^6 f^{(viii)}(\xi_3) \right\}. \quad (5)$$

$$f_N''(R_{m-2}) = \frac{1}{h^2} \left[\frac{3}{8} f_N(R_{m-5}) + 6f_N(R_{m-4}) - h^2 f_N''(R_{m-4}) - \frac{51}{4} f_N(R_{m-3}) - \frac{11}{2} h^2 f_N''(R_{m-3}) + 6f_N(R_{m-2}) + \frac{3}{8} f_N(R_{m-1}) \right] + \left\{ -\frac{23}{10080} h^6 f^{(viii)}(\xi_4) \right\} \quad (6)$$

$$f_N''(R_{m-1}) = \frac{1}{h^2} \left[\frac{3}{8} f_N(R_{m-4}) + 6f_N(R_{m-3}) - h^2 f_N''(R_{m-3}) - \frac{51}{4} f_N(R_{m-2}) - \frac{11}{2} h^2 f_N''(R_{m-2}) + 6f_N(R_{m-1}) + \frac{3}{8} f_N(R_m) \right] + \left\{ -\frac{23}{10080} h^6 f^{(viii)}(\xi_5) \right\}. \quad (7)$$

In each of Eqs. (3)-(7) quantities on the right hand sides within the curly brackets represent the error terms. The corresponding difference equations are obtained by substituting the values of second order derivatives from the differential equation (2) into these expressions. For continuing these solutions in the domain (Δ, R_∞) we need first order derivatives $f_N'(R)$ at Δ . These are computed from the difference formula

$$f_N'(R_m) = \frac{1}{84h} [-f_N(R_{m-4}) + 24f_N(R_{m-2}) - 128f_N(R_{m-1}) + 105f_N(R_m)] + \frac{2h}{7} f_N''(R_m) + \left\{ -\frac{4h^4}{105} f_N^{(v)}(\xi) \right\} \quad (8)$$

Here too, the quantity within curly brackets represents the error term. The solutions thus obtained in $(0, \Delta)$ are then continued over (Δ, R_∞) by Taylor's expansion method, as stated earlier, with stabilization after suitable steps [20].

III. RESULTS

In our present calculation for the equal-energy-sharing kinematics and 1eV, 0.5eV and 0.3eV excess energies, we have included 30 channels and have chosen $\Delta = 5$ a.u. (as in our previous calculation [12] for higher energies). Small variation of the value of Δ about the value chosen does not change the results. Here we need to choose R_∞ equal to 1000 a.u. for 1eV, 2000 a.u. for 0.5eV and 3000 a.u. for 0.3eV for smooth convergence of the asymptotic series solution and for smooth fitting with the asymptotic solution [12] in the equal energy sharing cases. For unequal energy sharing cases one may need to move to still larger distances. For going that far in the asymptotic domain a larger value of h (grid spacing) is preferable. Here we have chosen $h = 0.1$ a.u. up to Δ and a value 0.2 a.u. beyond Δ in all the cases. Accordingly a seven point scheme, as described above, is more suitable over a five point scheme used in our earlier calculation [12]

and hence we chose the above seven-point scheme in the present calculation. We included states with L up to 5. Values of L above 5 give insignificant contributions. The (l_1, l_2) pairs which have been included in our calculation are sufficient for convergence as found from the results of calculations with the inclusion of larger number of channels. All the computations were carried out on a 2 CPU SUN Enterprise 450 system with 512 MB RAM.

For each incident energy three sets of results with different geometry have been presented for the two outgoing electrons having equal energies. These are the constant - θ_{ab} geometry results, θ_a -constant geometry results and the results for symmetric geometry. For 1eV excess energy we have presented these results in figures 1(a), 1(b) and 1(c) respectively. The corresponding results for energy 0.5 eV are presented in figures 2(a), 2(b) and 2(c) respectively and the results for 0.3 eV have been presented in figures 3(a), 3(b) and 3(c) respectively. The bottom row of each of the figures 1(a), 2(a) and 3(a) corresponding to $\theta_{ab} = 150^\circ$ and $\theta_{ab} = 180^\circ$ are as in our earlier work [21] (though these are now calculated with different R_∞ values). This is merely to ensure completeness in the results presented and to compare our results with the semiclassical calculation of Deb and Crothers. For other geometries, unfortunately, neither experimental nor any theoretical results are available for comparison. The overall agreement between our results and those of Deb and Crothers [13] for $\theta_{ab} = 180^\circ$ and $\theta_{ab} = 150^\circ$ is highly encouraging. A little steeper rise of our results compared to those of Deb and Crothers [13] at 0° are in conformity with the general trends of our corresponding earlier results [12] at 2eV and 4eV excess energies. Our results for $\theta_{ab} = 120^\circ$ and 100° also appear reasonable when compared with the shapes of the corresponding results for 2 eV and 4 eV excess energy [12]. Unfortunately there are no experimental results for verification. The results for θ_a -constant geometry and those of symmetric geometry are also in very nice agreement in shapes, particularly for $\theta_a = -30^\circ$ and $\theta_a = -150^\circ$, with those for 2eV and 4eV excess energy cases (see Das *et al* [12]).

IV. CONCLUSION

From the results presented above it appears that the hyperspherical partial wave theory works satisfactorily at 1eV, 0.5eV and 0.3eV excess energies. We have already good results [12] for energies up to 30eV for various kinematic conditions. Calculations at a higher incident energy of 54.4eV are now in progress and we propose to present them in future. Another point to note is that in this approach exploration of the far asymptotic domain is

possible by increasing R_∞ to thousands of atomic units. All these suggest that the hyperspherical partial wave theory is capable of being developed into a successful method for (e, 2e) collisions.

Acknowledgments

S.P. gratefully acknowledges a research fellowship provided by CSIR.

-
- [1] C. Pan and A.F. Starace, Phys. Rev. Lett. **67**, 185 (1991); Phys. Rev. A **45**, 4588 (1992).
 - [2] S. Jones, D.H. Madison, and M. K. Srivastava, J. Phys. B **25**, 1899 (1992).
 - [3] T. N. Rescigno, M. Baertschy, W. A. Isaacs, and C. W. McCurdy, Science **286**, 2474 (1999).
 - [4] M. Baertschy, T. N. Rescigno, W. A. Isaacs, X. Li, and C. W. McCurdy, Phys. Rev. A **63**, 022712 (2001).
 - [5] M. Baertschy, T. N. Rescigno, and C. W. McCurdy Phys. Rev. A **64**, 022709 (2001).
 - [6] J. Röder, H. Ehrhardt, C. Pan, A. F. Starace, I. Bray, and D. V. Fursa, Phys. Rev. Lett. **79**, 1666 (1997).
 - [7] J. Röder, M. Baertschy, and I. Bray, Phys. Rev A **67**, 010702(R) (2003).
 - [8] J. Röder, J. Rasch, K. Jung, C. T. Whelan, H. Ehrhardt, R. J. Allan, and H. R. J. Walters, Phys. Rev. A **53**, 225 (1996).
 - [9] I. Bray, D. A. Konovalov, I. E. McCarthy, and A. T. Stelbovics Phys. Rev. A **50**, R2818 (1994).
 - [10] I. Bray, J. Phys. B **32**, L119 (1999) ; 2000 J. Phys. B **33**, 581 (2000).
 - [11] I. Bray, J. Phys. B **33**, 581 (2000).
 - [12] J. N. Das, S. Paul, and K. Chakrabarti, Phys. Rev. A **67**, 042717 (2003).
 - [13] N. C. Deb and D. S. F. Crothers, Phys. Rev. A **65**, 052721 (2002).
 - [14] P. Selles, L. Malegat, and A. K. Kazansky, Phys. Rev. A **65**, 032711 (2002).
 - [15] J. N. Das, Pramana- J. Phys. **50**, 53 (1998).
 - [16] P. G. Burke and W. D. Robb, Adv. At. Mol. Phys. **11**, 143 (1975).
 - [17] J. N. Das, Phys. Rev. A **64**, 054703 (2001).
 - [18] J. N. Das, J. Phys. B **35**, 1165 (2002).
 - [19] C. D. Lin, Phys. Rev. A **10**, 1986 (1974).
 - [20] B. H. Choi and K. T. Tang, J. Chem. Phys. **63**, 1775 (1975).
 - [21] J. N. Das, S. Paul, and K. Chakrabarti, AIP Conference Proceedings **697**, 82 (2003).
-

Figure Captions

Figure 1(a). TDCS for coplanar equal-energy-sharing constant Θ_{ab} geometry at 1eV excess energy above threshold. Continuous curves, present results ; dashed-curves, semiclassical results of Deb and Crothers [13]

Figure 1(b). TDCS for coplanar equal-energy-sharing geometry at 1eV excess energy above threshold for fixed θ_a and variable θ_b of the out going electrons.

Figure 1(c). TDCS for coplanar equal-energy-sharing with two electrons emerging on opposite sides of the direction of the incident electron with equal angle θ_a at 1eV excess energy above threshold.

Figure 2(a). TDCS for coplanar equal-energy-sharing constant Θ_{ab} geometry at 0.5eV excess energy above threshold. Continuous curves, present results ; dashed-curves, semiclassical results of Deb and Crothers [13]

Figure 2(b). TDCS for coplanar equal-energy-sharing geometry at 0.5eV excess energy above threshold for fixed θ_a and variable θ_b of the out going electrons.

Figure 2(c). TDCS for coplanar equal-energy-sharing with two electrons emerging on opposite sides of the direction of the incident electron with equal angle θ_a at 0.5eV excess energy above threshold.

Figure 3(a). TDCS for coplanar equal-energy-sharing constant Θ_{ab} geometry at 0.3eV excess energy above threshold. Continuous curves, present results ; dashed-curves, semiclassical results of Deb and Crothers [13]

Figure 3(b). TDCS for coplanar equal-energy-sharing geometry at 0.3eV excess energy above threshold for fixed θ_a and variable θ_b of the out going electrons.

Figure 3(c). TDCS for coplanar equal-energy-sharing with two electrons emerging on opposite sides of the direction of the incident electron with equal angle θ_a at 0.3eV excess energy above threshold.

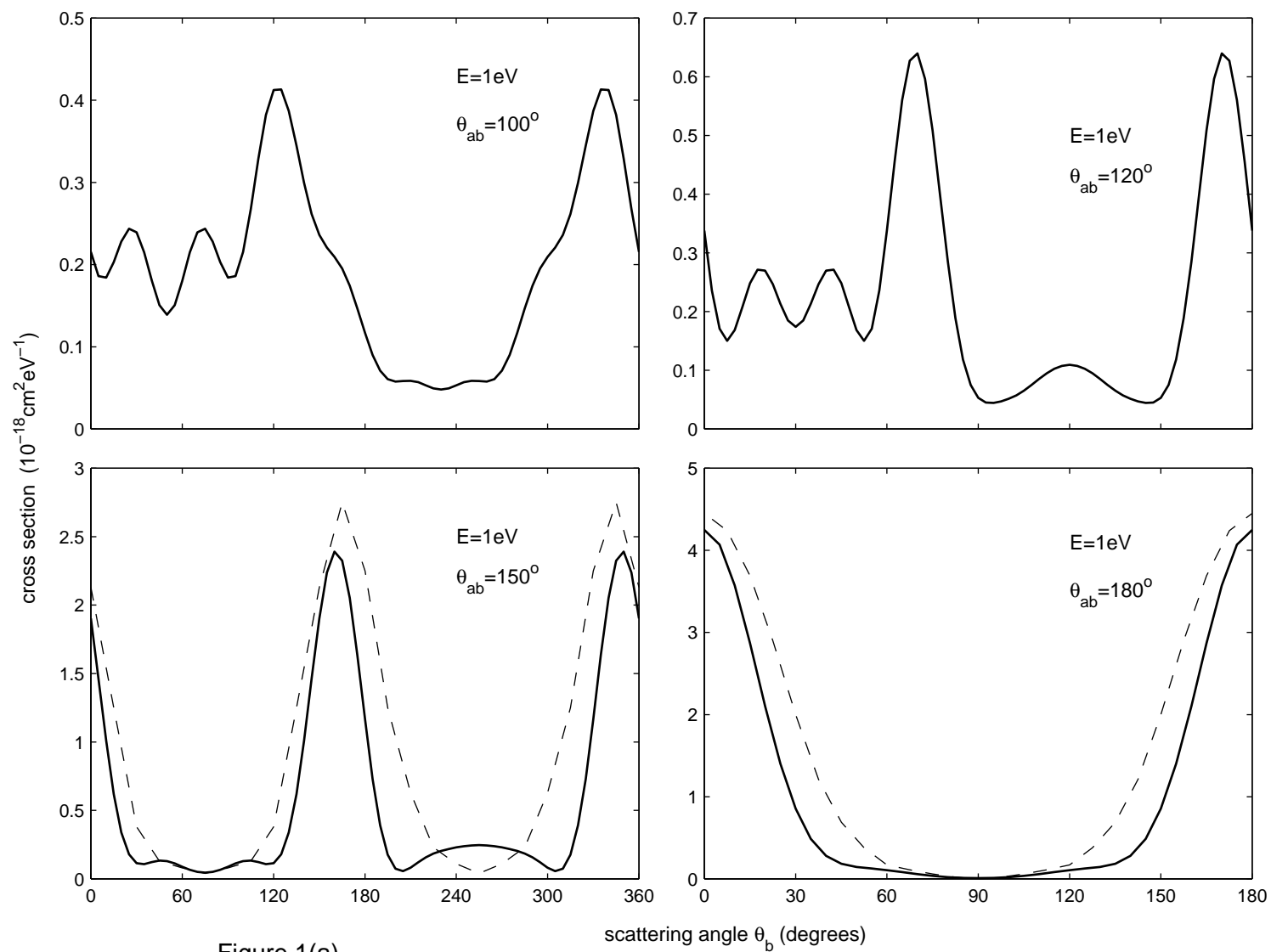


Figure 1(a)

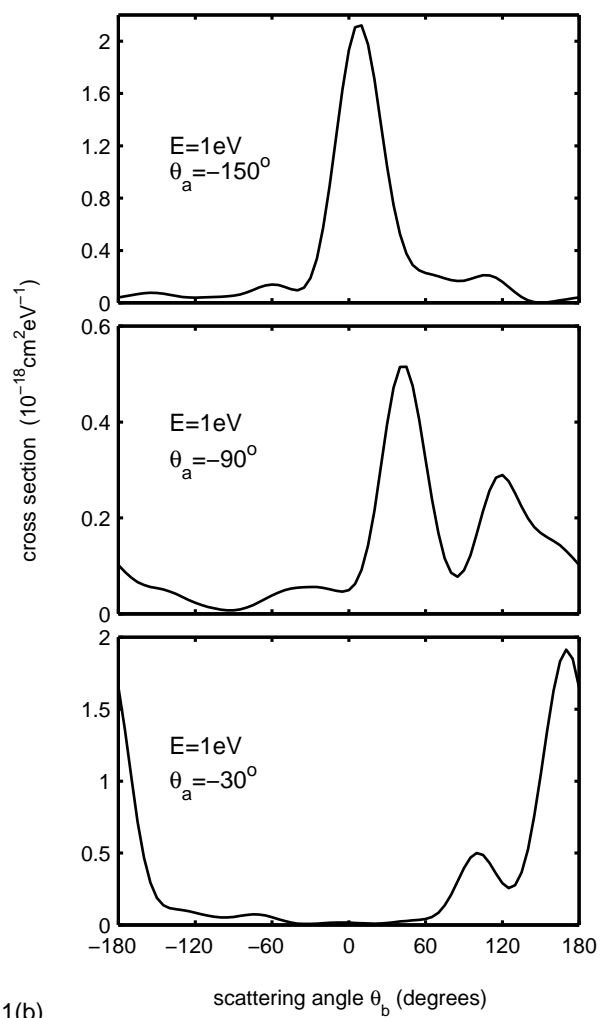


Figure 1(b)

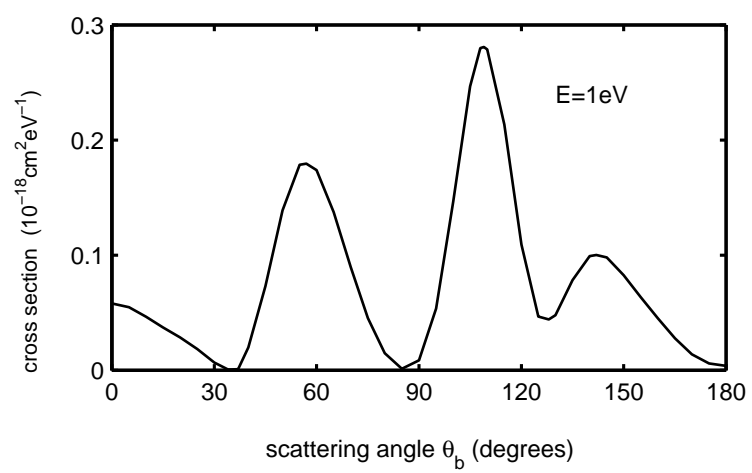


Figure 1(c)

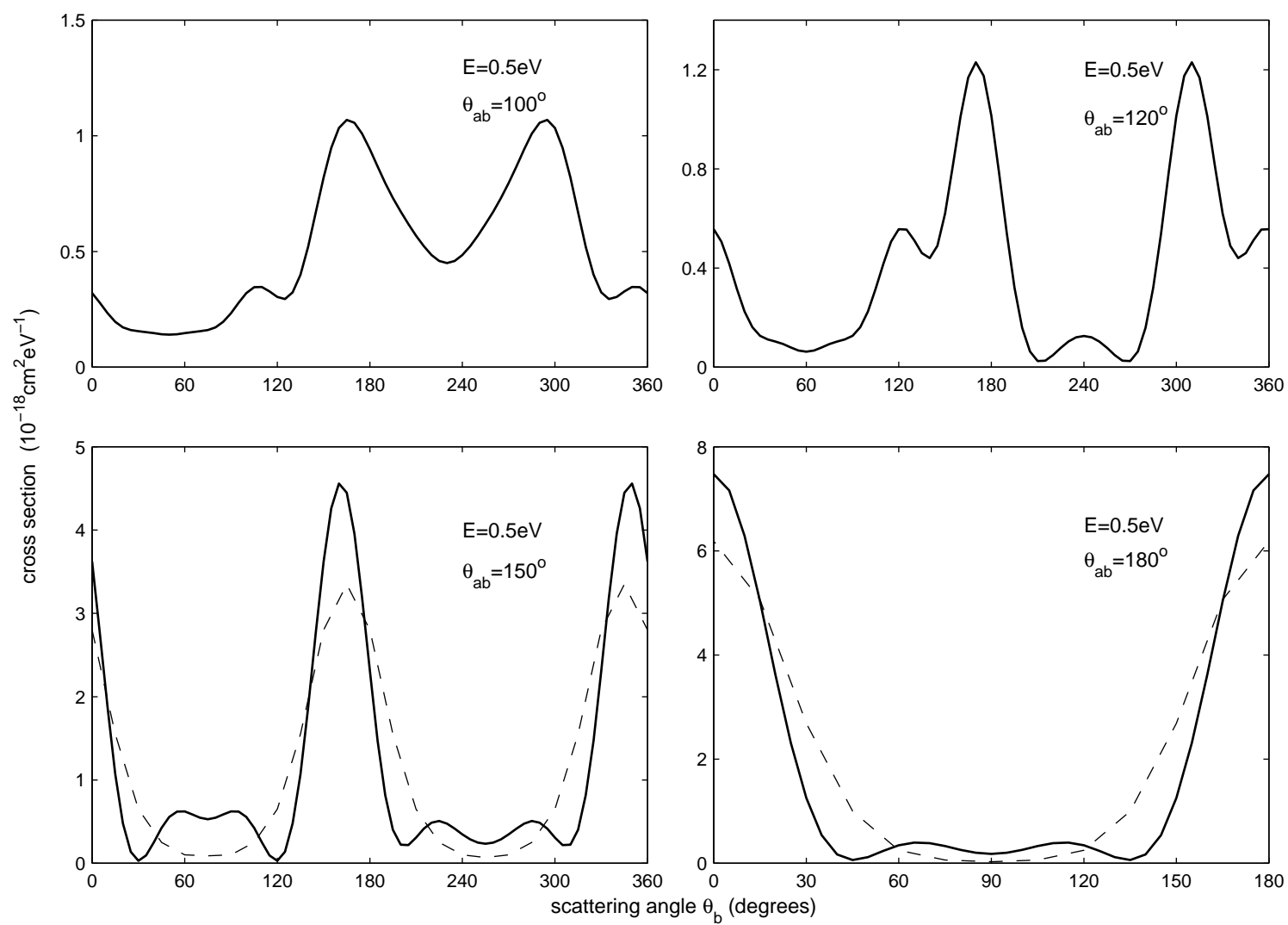


Figure 2(a)

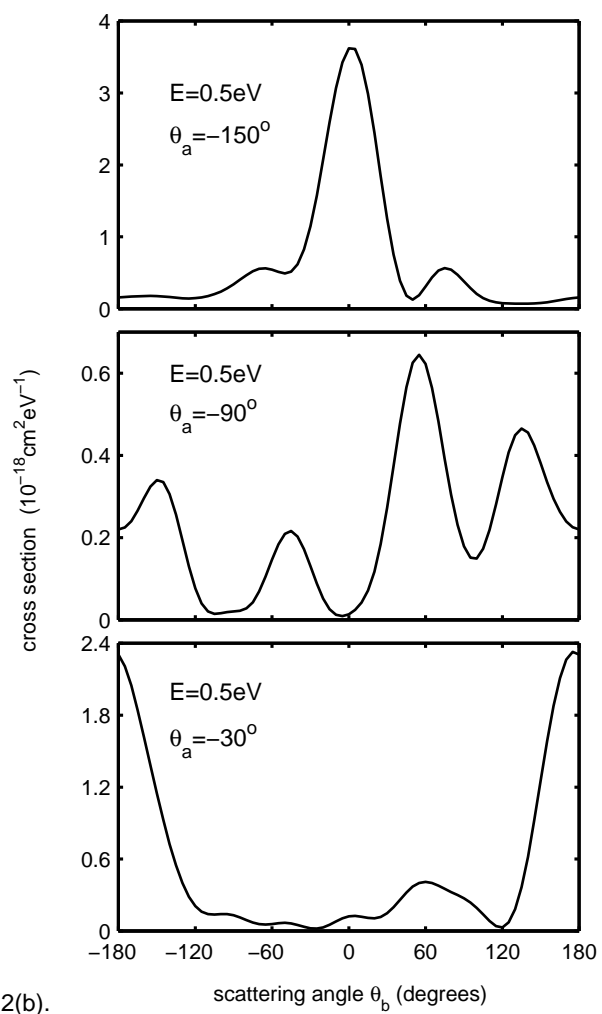


Figure 2(b).

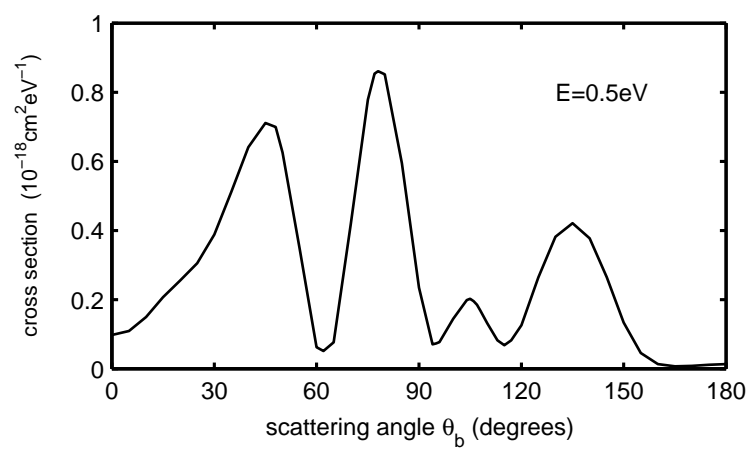


Figure 2(c)

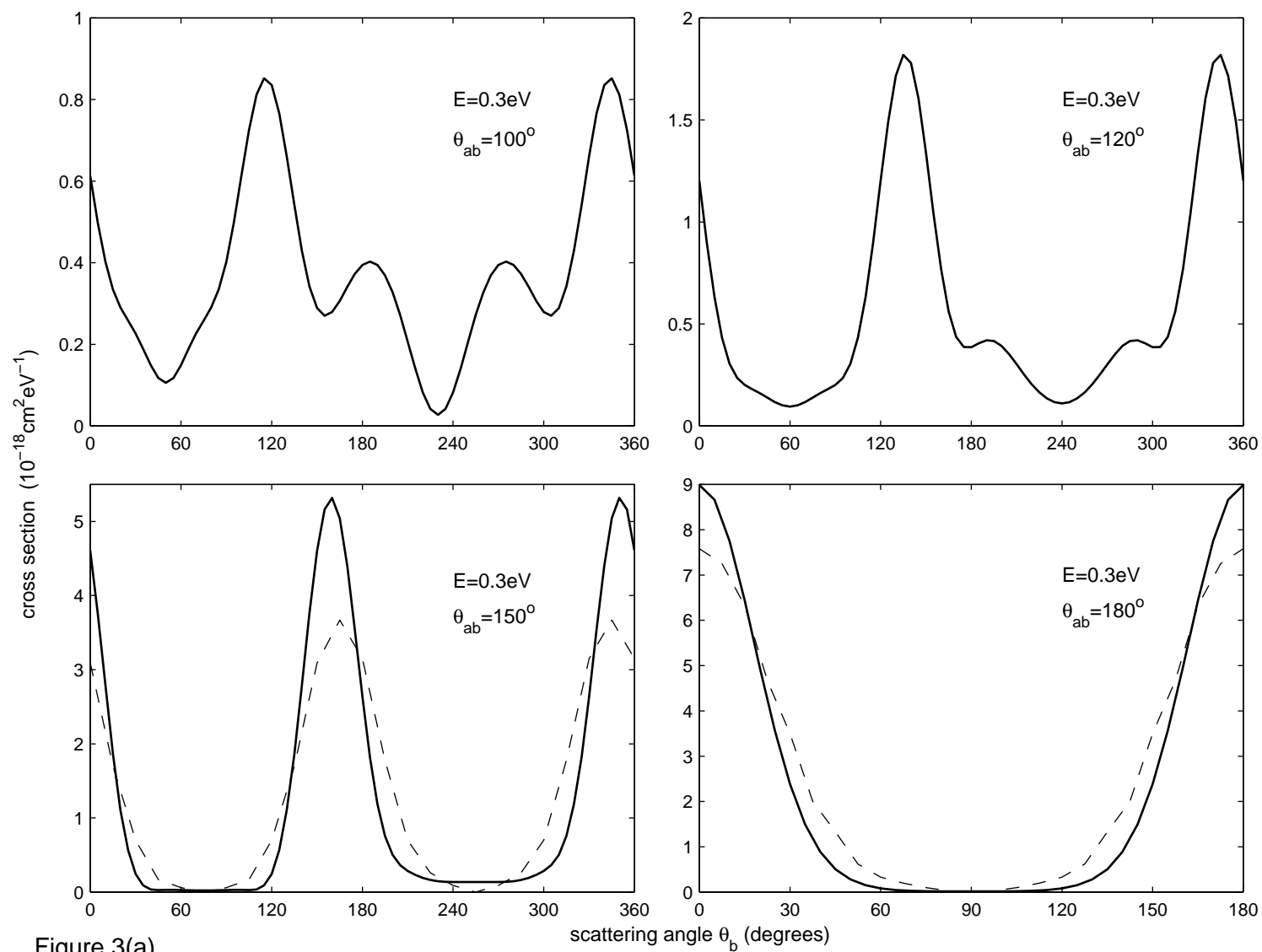


Figure 3(a)

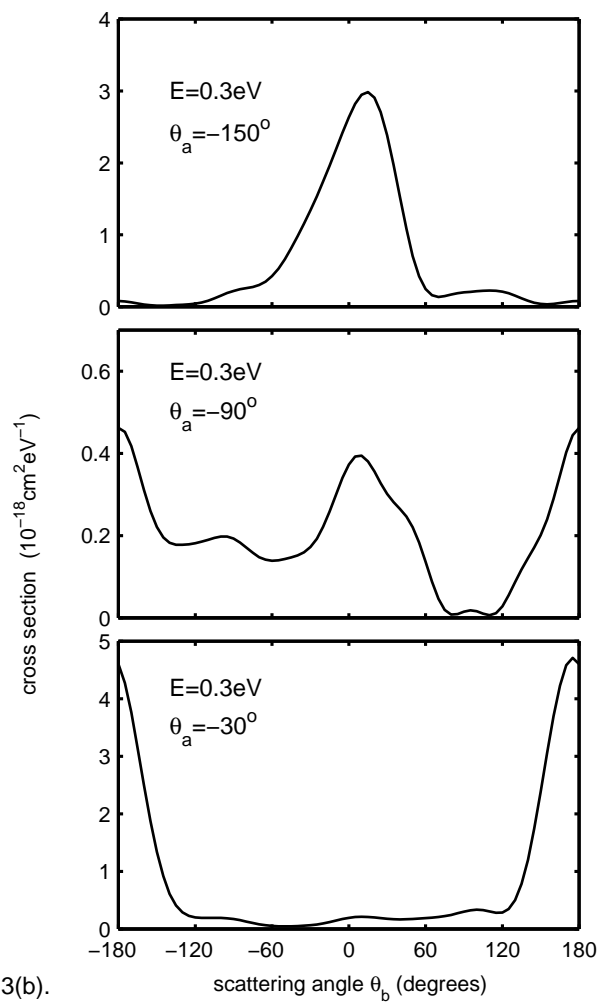


Figure 3(b).

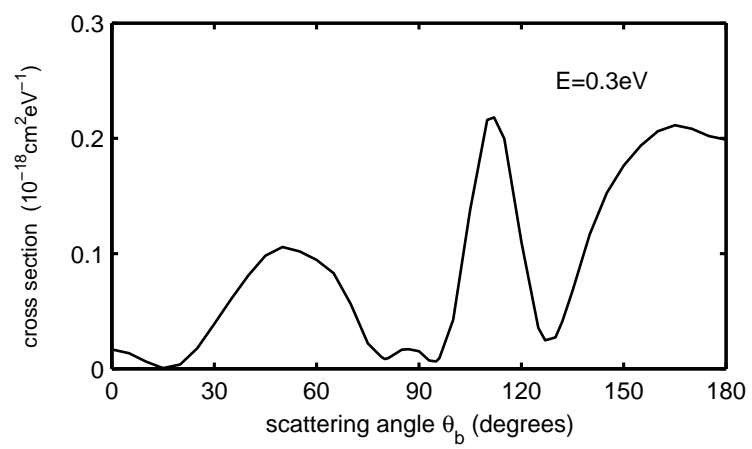


Figure 3(c)